

# Experimental Analysis of Micro-Wind Turbine Performance: Blade Geometry and Wind Speed Interactions

Dattu Balu Ghane\*, Vishnu D Wakchaure

Amrutvahini College of Engineering, Sangamner, Ahilyanagar, India. Corresponding Author's Email: dattu.ghane@gmail.com

## Abstract

Micro-wind turbines (MWTs) are increasingly recognized as a viable solution for decentralized renewable energy generation. This is especially true in regions with low to moderate wind speeds. These conditions necessitate experimental investigations into their aerodynamic performance and optimization. This study examines the power generation of MWTs with varying blade radii (200mm, 220mm, 240mm, and 260mm) across wind speeds ranging from 3 to 12 m/s. It also covers different blade configurations, including an analysis of the effect of blade number. The results highlight the non-linear relationship between wind speed and power output, with significant increases observed at higher wind velocities. An experimental test setup was developed to analyze the performance of MWTs under controlled conditions. The setup includes a wind tunnel capable of generating wind speeds. Precision measurement instruments record wind speed, torque, and rotational speed. A modular turbine mount, as well as a modular turbine mount, allows testing of blades with varying radii and configurations. The results demonstrate that power generation increases with wind speed for all tested blade radii and configurations. A pronounced rise occurs at higher wind velocities, confirming a non-linear relationship between wind speed and power output. This highlights the influence of blade radius and number of blades on overall turbine performance.

**Keywords:** Blade Design Optimization, Low Wind Speed Optimization, Micro-Wind Turbines, Renewable Energy, Wind Energy Systems.

## Introduction

The rapid depletion of fossil fuel sources and the environmental concerns that accompany them necessitate the use of renewable energy sources for power generation (1). Due to its global accessibility and capacity to generate electricity without emitting greenhouse gases, wind energy is among the most promising renewable energy sources (2). Micro wind turbines (MWTs) have emerged as a viable solution for decentralized power generation, particularly in urban and residential settings where conventional large-scale turbines are impractical (3). These small-scale turbines are engineered to effectively capture wind energy at reduced speeds, offering a sustainable and environmentally friendly alternative to conventional fossil fuel-based power sources (4). The integration of MWTs into the energy grid not only promotes energy security and resilience in diverse environments but also assists in the reduction of greenhouse gas emissions (5). MWTs are classified into two categories: horizontal-axis wind turbines (HAWTs) and vertical-axis wind turbines (VAWTs). Each type is optimized for specific

environmental conditions and applications. VAWTs are well-suited for urban environments due to their superior performance in turbulent and multidirectional wind environments, while HAWTs are generally more efficient in stable, high-wind conditions (6). Flexible blades that can adjust to changing wind speeds have been incorporated into MWT technology in recent years, which has significantly improved energy capture and efficiency (7). There is a wide range of turbine blade shapes, including straight blades, curved designs such as Darrieus and Gorlov types, and bio-inspired shapes that enhance aerodynamic efficiency (8). The recent development of flexible or morphing blades in MWTs has resulted in improved energy capture and efficiency by adapting to variable wind conditions (7). The broader adoption of sustainable energy solutions are significantly facilitated by these innovations, which render MWTs more efficient, cost-effective, and suitable for a variety of renewable energy applications. Blade design and material selection have been the primary focus of recent advancements in the optimization of

This is an Open Access article distributed under the terms of the Creative Commons Attribution CC BY license (<http://creativecommons.org/licenses/by/4.0/>), which permits unrestricted reuse, distribution, and reproduction in any medium, provided the original work is properly cited.

(Received 21<sup>st</sup> September 2025; Accepted 31<sup>st</sup> December 2025; Published 31<sup>st</sup> January 2026)

MWTs to optimize power output and efficiency. A dynamically morphing VAWT that optimizes blade shapes based on azimuthal angle and Tip Speed Ratio (TSR) using CFD-based optimization and Free-Form Deformation (FFD) algorithms was developed by Baghdadi (9). This technique significantly enhanced power output when used with a NACA 0021 airfoil. A comprehensive methodology was built that integrates a GA with CFD to optimize wind turbine blades (10). The NACA 4412 was outperformed by their optimized airfoil, which resulted in a 5.244 m blade for a 5-kW turbine. This blade achieved a maximum coefficient of performance ( $C_p$ ) of 0.4658 at a TSR of 6, indicating superior performance in a variety of conditions. The BEM theory was employed and Q-blade software to optimize small HAWT blades by the Umar (11). They discovered that SG6043 airfoils at a TSR of 6 generated the highest power coefficients and outputs, reaching up to 245.09 W. Consequently, they are well-suited for off-grid applications and low-wind-speed regions. The optimization of materials, specifically using PLA and ABS to design an efficient airfoil blade for a micro-HAWT (12). In wind tunnel tests, the blade with 79.77% PLA infill achieved a power output of 97 W, surpassing the PSO algorithm's performance, because of their FEA and MFO algorithm optimization. The 3D micro-HAWT blade design was optimized by using CFD analysis and the MOGA method (13). The study focused on the distribution of twist angle and chord length, resulting in a 3.6% efficiency improvement at a TSR of 3.4. Using the Taguchi method, optimized the blade geometry of ducted micro-HAWTs, resulting in a 39.4% increase in the maximum  $C_p$  with optimal parameters of 8 blades, 60% solidity, and a 30° pitch angle (14). Together, these studies emphasize the progress made in the optimization of MWTs with advanced algorithms, innovative blade designs, and material enhancements, thereby offering a comprehensive approach to enhancing the efficiency and effectiveness of wind energy solutions.

Scientists have examined a variety of composite materials for MWT blades, such as carbon fiber-reinforced composites for improved bending strength and glass fiber-reinforced composites for cost-effectiveness and improved mechanical properties (15, 16). Furthermore, glass fiber-reinforced polypropylene nanocomposites

containing MWCNTs have exhibited substantial reductions in blade deflection and an increase in tensile strength, rendering them suitable for both small and larger wind turbine blades (17).

Recent developments in the field of MWTs have been characterized by a plethora of experimental and numerical studies that concentrate on the optimization of blade design, materials, and performance under a variety of conditions. The evaluation of the wind resource characteristics for MWTs on noise barriers was conducted by Chrysochoidis-Antsos (18). They discovered substantial variations in wind speed and energy yield that were dependent on the height of the barrier and the direction of the flow. This evaluation has the potential to result in cost reductions in the Levelized Cost of Energy. Using both experimental and CFD simulations, Eltayesh. demonstrated that turbines with fewer blades (three-blade configuration) achieve higher power coefficients than those with more blades (19). The 300W fiberglass wind rotor blade that Kadhim et al. developed for low-speed winds in Iraq was successfully tested in practical applications (20). The blade was simulated using SolidWorks and Q-blade. An analysis of low Reynolds number airfoils using CFD and wind tunnel experiments was conducted by Seifi Davari (21). They identified significant impacts on vortex shedding and Reynolds numbers, which were then, analyzed for their lift coefficient ratios. The micro wind turbines typically operates in the 10000–100000 Reynolds number range due to small rotor size and low wind speeds. In this range of Reynolds number, viscous effects, early flow separation and reduced lift-to-drag ratios strongly influence starting torque, power coefficient and optimal tip speed ratio. An exhaust fan cum micro wind turbine (EFCMWT) developed, that generated a maximum power output of 1.2167 watts, underscoring its potential to lessen carbon footprints (22). Using material innovations as a foundation, conducted a comparison of polymer-based wind blades composed of PLA and ABS materials (23). They discovered that PLA outperformed ABS in terms of stress, strain, and deformation, rendering it the optimal choice for low wind speed applications. Together, these studies underscore the ongoing endeavors and advancements in the enhancement of the efficiency, material selection, and overall performance of MWTs through both experimental

and numerical methods. Acoustically, horizontal turbines also produce less low-frequency noise due to a smoother flow of the aerodynamic blades and less turbulence around the trailing edge (24). Moreover, HAWTs have a technological advantage in that decades of optimization of their design have resulted in standardized designs, stable control systems, and predictable performance in different wind regimes (25). Although relative to the prior studies, there are remarkable improvements in the small wind turbines designs, there is still the dearth of knowledge on how the several designs attributes, including blade radii, configuration, and number of blades will affect the power coefficient at different wind speeds especially in the Cut-in and rated wind speed regimes. The performance of micro-wind turbines (MWTs) is analyzed in this research paper based on the blade radii, configurations, and number of blades with respect to the operational conditions. Several experiments were performed to evaluate the power performance at various wind speeds of 3m/s to 12m/s, with indications of how the various design features would affect the aerodynamic performance and electricity production.

## Methodology

### Experimental Test Setup and Procedure

The experimental setup for testing the horizontal axis micro wind turbine was designed to evaluate

its performance under varying wind speeds, blade radii, and blade configurations. The following equipment was used: an axial flow fan with adjustable speed to generate wind, a wind tunnel, a horizontal axis wind turbine, a digital anemometer, a non-contact type turbine speed sensor, a power meter, and a data acquisition system. The axial flow fan, controlled by a variable frequency drive (VFD), was installed at one end of the wind tunnel to produce adjustable wind speeds ranging from 3 to 12 m/s. This setup allowed for precise control of the wind conditions within the tunnel. The horizontal axis micro wind turbine was mounted securely inside the wind tunnel, ensuring optimal alignment with the airflow. Figure 1 shows that the micro wind turbine blades with varying radius (200mm, 220mm, 240mm and 260mm) are 3D printed using thermoplastic polyurethane (TPU) for flexibility and durability. The images display the blades from multiple angles: front, back, and both sides. The aerodynamic design and structural features of the blades are presented in these perspectives in detail. We specifically chose the varying radii of the blades to assess the impact on power generation efficiency of the turbine. The design is designed for wind energy capture maximization and thus to improve the overall performance of the turbine in the experimental setup.

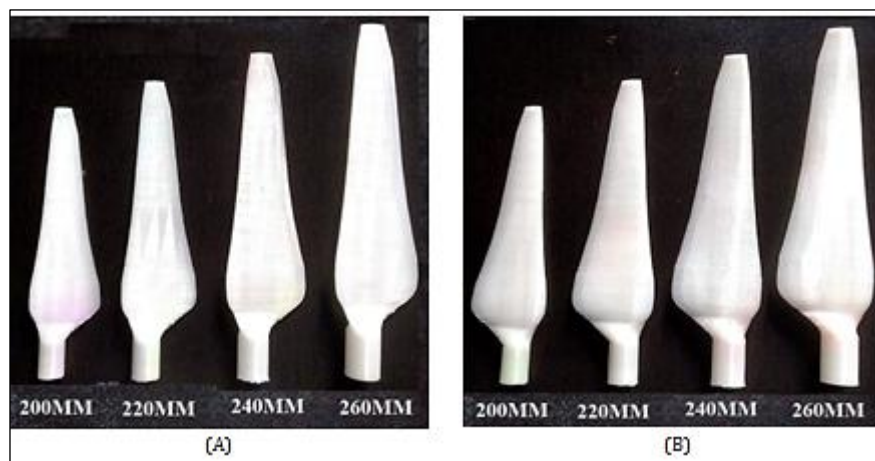


**Figure 1:** Actual Photographs of the Turbine Blades Used in the Study as (A) Front Side, (B) Back Side

A digital anemometer was placed at the same height as the turbine blades to accurately measure the wind speed within the tunnel. A non-contact type turbine speed sensor was aligned with the turbine shaft to measure its rotational speed

(RPM) without physical contact, thus avoiding any interference with the turbine's operation. The power meter was connected to the turbine's electrical output to measure the power generated during the tests. All these measurement

instruments were integrated with the data acquisition system, which enabled real-time monitoring and recording of wind speed, turbine speed, and power output. The experiment was conducted under the following test conditions: wind speeds varying from 3 to 12 m/s, blade radii of 0.2m, 0.22m, 0.24m, and 0.26m, and turbine configurations with 3, 4, 5, and 6 blades. For each test condition, the wind speed was adjusted incrementally using the VFD, and the corresponding turbine performance metrics were recorded by the data acquisition system. The

measurements were repeated three times for each combination of wind speed, blade radius, and blade number to ensure accuracy and repeatability. This comprehensive experimental procedure allowed for a detailed assessment of the micro wind turbine's performance, providing valuable insights into the effects of different operational parameters on power generation efficiency. The data collected were analyzed to evaluate the  $C_p$  of turbine and power generation under various conditions.

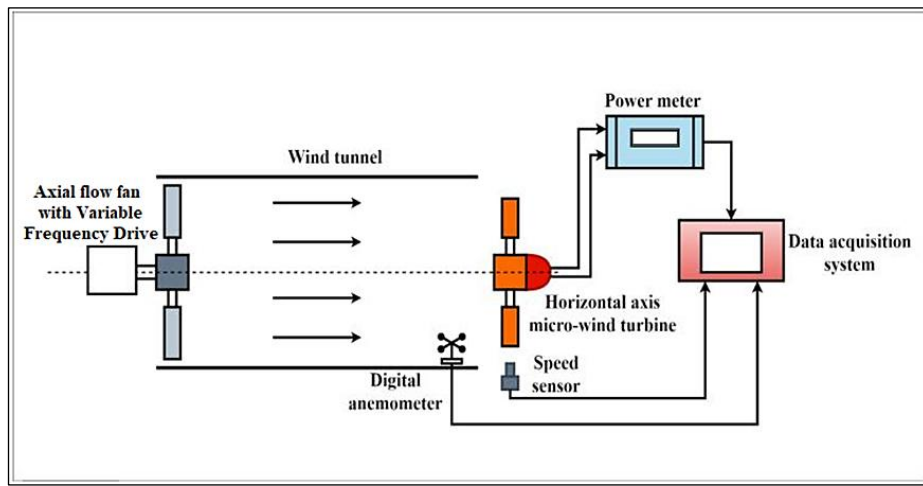


**Figure 2:** Experimental Test Setup

## Instrumentation

### Anemometer

In the present research, the KE-856A commercial wind speed measuring device was utilized due to its high accuracy to measure wind speed within the controlled environment of the wind tunnel. The KE-856A measures wind speed in the range of 0.3 to 45 m/s with an accuracy of  $\pm 3\%$  and a resolution of 0.01 m/s, but it also measures wind temperature from 0°C to 45°C. Additionally, it can display air, making it a versatile tool for detailed wind analysis. The anemometer was strategically positioned at the same height as the micro-wind turbine to ensure precise and representative wind speed readings that directly impact the turbine blades. Integrated with a data acquisition system, the KE-856A facilitated real-time monitoring and logging of wind speed, temperature, and air volume data. The device can store 600 groups of wind reading data, which can be downloaded and analyzed via PC using the provided USB cable and customized computer software. The KE-856A provides high sensitivity, enhanced with low-friction bearing, ensures accurate detection of

airflow, which is critical for the reliability and validity of the experimental data. Figure 2 shows the digital anemometer used for the study.

### Speed Sensor

In the present research, a high-precision, non-contact speed sensor (DT-2234C) was employed to measure the rotational speed of the micro-wind turbine. The speed sensor was mounted on a tripod stand at an appropriate height and distance alongside rotating turbine to measure real-time turbine speed. Utilizing laser or infrared technology, this sensor provided accurate RPM measurements without physical contact, minimizing interference and mechanical wear. With a measurement range from 2.5 to 99,999 RPM and an accuracy of  $\pm 0.05\% + 1$  digit, the sensor ensured reliable and precise data collection. The resolution was 0.1 RPM for speeds below 1,000 RPM and 1 RPM for speeds at or above 1,000 RPM. Integrated with the data acquisition system, the speed sensor facilitated real-time monitoring and recording of the turbine speed across various wind speeds and blade configurations. This integration enabled the synchronization of RPM data with

wind speed, providing a comprehensive dataset for analysis. The continuous data logging capability of the system allowed for detailed performance evaluation and optimization of the micro-wind turbine under different operating conditions.

### **Power Meter**

In the present research, a precision power meter was utilized to measure the electrical power generated by the micro-wind turbine. The power meter was connected to the output terminals of the turbine to accurately capture the voltage and current produced during the experiments. This device was crucial for providing real-time measurements of the turbine's electrical output, allowing for immediate assessment of performance under varying wind speeds, blade radii, and blade configurations. The power meter was integrated with the data acquisition system, which enabled continuous recording and synchronization of power output data with other critical parameters such as wind speed and turbine rotational speed (RPM). This setup facilitated comprehensive data collection and ensured that all relevant performance metrics were accurately logged for subsequent analysis. The high accuracy and resolution of the power meter were essential for understanding the efficiency of the turbine and for making precise comparisons across different test conditions.

### **Data Acquisition System**

In this research, an advanced data acquisition system (DAS) was employed to measure and collect critical performance data of the micro-wind turbine. The DAS was integral to the experimental setup, enabling real-time monitoring and recording of key parameters, including power output, turbine rotational speed (RPM), and wind speed. The DAS was interfaced with a power meter to accurately capture the electrical output of the turbine, while a non-contact turbine speed sensor provided precise RPM measurements. Additionally, a digital anemometer supplied continuous wind speed data. Integrating these instruments into the DAS ensured synchronized and comprehensive data collection, facilitating detailed analysis of the turbine's performance under various operational conditions.

### **Axial Flow Fan with VFD**

In the present research, an axial flow fan equipped with a variable frequency drive (VFD) was utilized to generate variable wind speeds within the wind

tunnel. The VFD allowed precise control of the rotational speed of the fan, enabling the creation of consistent and adjustable wind speeds ranging from 3 to 12 m/s. This capability was crucial for simulating different wind conditions and ensuring the accuracy and reliability of the experimental data. By adjusting the RPM of the fan through the VFD, the wind speed was systematically varied, and performance of the micro-wind turbine was assessed under diverse scenarios. This setup provided a controlled environment essential for evaluating the effects of different blade radii and blade numbers on the power output of turbine, rotational speed, and overall efficiency.

### **Wind Tunnel**

In the present research, a wind tunnel was employed to create a controlled environment for testing the micro-wind turbine. The wind tunnel allowed for consistent and reproducible wind conditions, essential for evaluating the performance of the turbine across various scenarios. By generating a uniform airflow, the wind tunnel ensured that the wind speed, direction, and turbulence levels remained stable throughout the experiments. This stability was critical for accurately measuring the power output of the turbine, rotational speed (RPM), and other performance metrics under different wind speeds, blade radii, and blade configurations. The controlled setting of wind tunnel enabled precise manipulation of test conditions, facilitating detailed analysis and comparison of the turbine efficiency and behaviour in response to changes in operational parameters. Overall, the wind tunnel played a pivotal role in providing the consistent and controlled wind environment necessary for the comprehensive evaluation of the performance of the micro-wind turbine.

### **Repeatability Test and Uncertainty**

#### **Measurement**

A repeatability test was conducted to ensure the reliability and consistency of the experimental measurements obtained for the MWT across varying configurations. The repeatability test involved repeating the measurements under identical conditions multiple times to estimate the precision of the data. Key parameters were measured repeatedly to assess the variation between successive trials.

Measurement of uncertainty is an imperative step for enumerating the potential variations in

measured values emerging from underlying inaccuracies in measurement instruments, experimental setups, and environmental conditions. In this study, standard uncertainty (U) and the uncertainties associated with key parameters, including air density ( $\rho$ ), swept area ( $A_s$ ), air velocity ( $V$ ), and turbine blade speed (N)

were systematically evaluated for the MWT across different configurations. This analysis provides a complete insight of the measurement inconsistency and ensures the reliability of the experimental results. Table 1 represents uncertainty in the measurement of these measured quantities.

**Table 1:** Measurement of Uncertainty

Parameter	Measured Value	Uncertainty	Percentage Uncertainty (%)
Air Density ( $\rho$ )	1.225 kg/m <sup>3</sup>	±0.02 kg/m <sup>3</sup>	1.63
Swept Area ( $A_s$ )	0.5 m <sup>2</sup>	±0.01 m <sup>2</sup>	2.00
Air Velocity (V)	10 m/s	±0.3 m/s	3.00
Turbine Speed (N)	1500 rpm	±20 rpm	1.33

The total uncertainty in the measurement is calculated by equation [1].

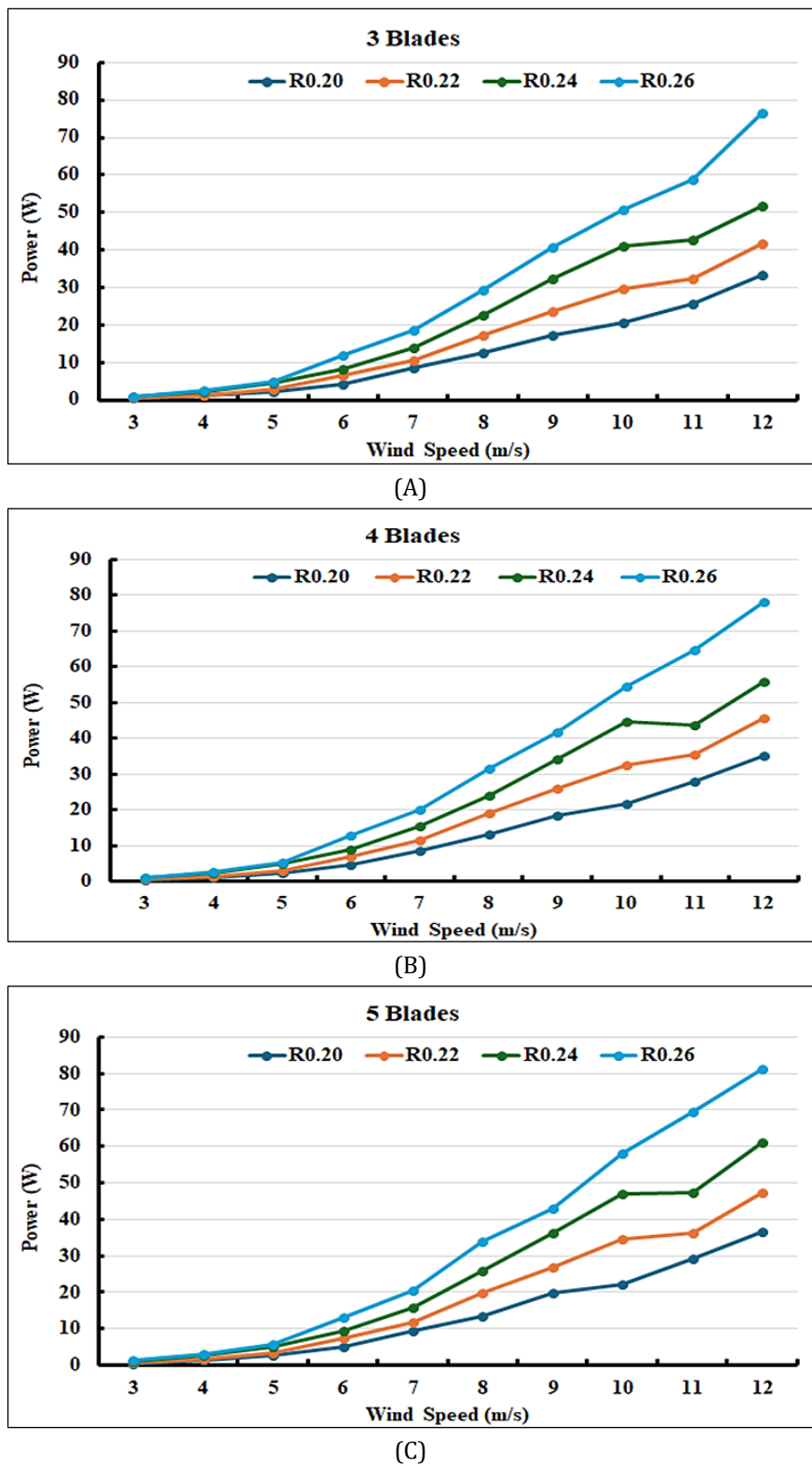
$$\text{Total uncertainty} = \sqrt{U\rho^2 + UA_s^2 + UV^2 + UN^2} = \pm 4.17\% \quad [1]$$

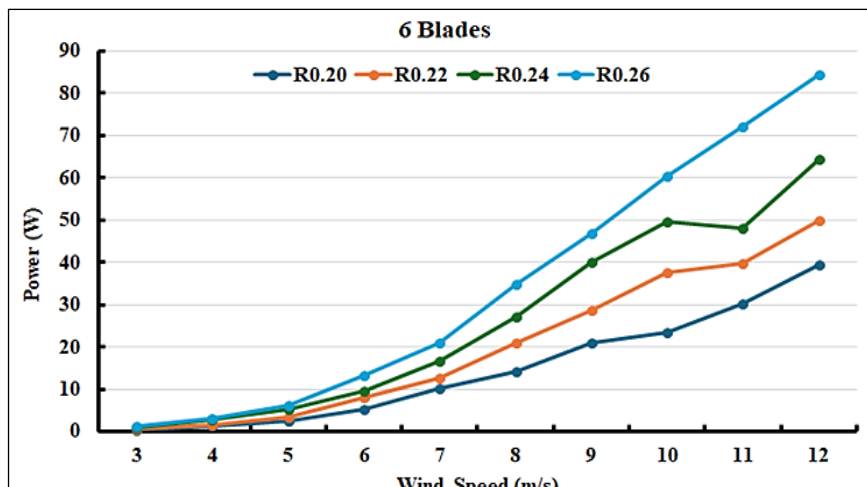
The total uncertainty in the measurement is within the permissible range ( $\pm 5\%$ ). The results demonstrated minimal variation, with deviations well within acceptable limits, confirming the repeatability of the experimental setup.

## Results and Discussion

The power generation from the MWT with varying blade radii (200mm, 220mm, 240mm and 260mm) over wind speeds ranging from 3-12 m/s for varying blade configurations are demonstrated in the Figure 3(A) and 3(B). It is obvious from Figures 3(A-D) that the power generation increases with increasing wind speed for all blade configuration and blade radii. The rise in power generation is prominent at higher wind velocities, exhibiting non-linear relationship between wind speed and power generation. This is attributed to the fact that, the power generation is proportional to the cube of the wind speed ( $V^3$ ). Moreover, increasing the blade radii had a positive effect on power generation. A MWT with higher blade radii generates higher power at a given wind speed and blade count. This is because, turbine with higher radii acquires more wind energy on account of increased swept area. For instance, 20% increasing the blade radii (200 to 240 mm) results in 44% rise

in swept area ( $A_s$ ) of the turbine. At low wind speeds, the difference between the power generated by smallest (200mm) and largest (260mm) radii turbine is very low, which increases substantially at higher wind speeds. Namely, for a 3 blade configuration, the turbine produces 2.44 times more power with a 260mm radii turbine compared to 200mm radii turbine. Additionally, increasing the number of blades provides higher starting torque which enables turbine to rotate and generate power even at low wind speeds. Additional blades offers a higher surface area that enhances the ability to harness wind energy at low wind speeds. As a consequence, increased number of blades increased power generation, especially at lower wind velocities. With increased wind speed, the aerodynamic drag over the blade surface increases substantially. For turbines with high blade count, aerodynamic drag becomes significant, reducing the efficiency of energy conversion. Furthermore, higher blade count leads to airflow interference over adjoining blades disturbing the steady flow of air. As a result, the difference in power generation between turbines with varying blade number becomes insignificant but still favors configurations with more blades.





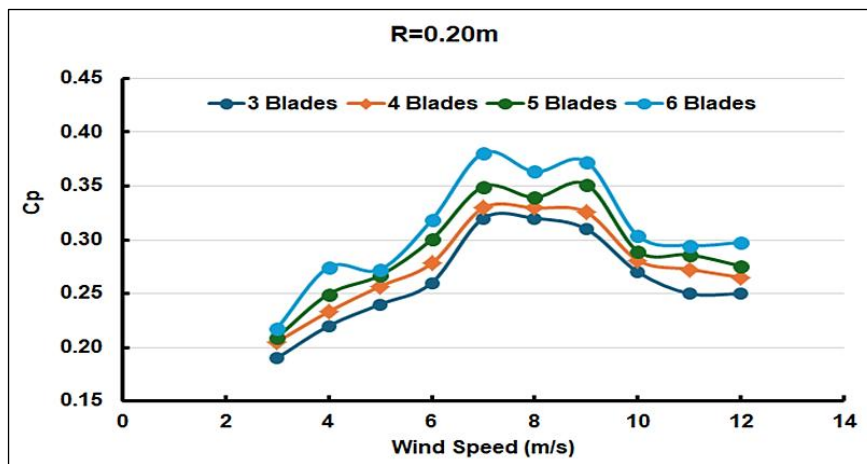
(D)

**Figure 3: Power Generated by Micro-Wind Turbine with Varying Blade Radii with (A) 3-blade, (B) 4-blade, (C) 5-Blade and (D) 6-Blade Configuration Power Generation**

### Coefficient of Performance (Cp)

Deviation of Cp of a MWT with varying blade radii and varying blade numbers over a range of wind speeds (3-12 m/s) are shown in Figures 4(A-D). At lower wind speeds, Cp is lower which tend to increase with increased wind speed to an extent and starts to decline at higher wind speeds. The turbine demonstrates same trend for Cp irrespective of blade configuration and blade radii. At low wind speeds, a major portion of the wind energy is utilized to overcome mechanical friction and inertia. As a result, the turbine produces less power with lower Cp value. With increased wind velocity, a higher portion of wind energy is converted to useful power with increased coefficient of performance. Irrespective of the blade radii and blade count, turbine provides higher efficiency in the wind speed range of 6-8 m/s with higher value of Cp. Increasing the blade

count and blade radii have positive impact on the Cp across all wind speeds owing to the increased swept area and blade surface area. For example, for a turbine with 200mm blade radii, the average coefficient of performance values over all wind speeds recorded are 0.263, 0.278, 0.292 and 0.31 for 3, 4, 5 and 6 blade configurations respectively. Similarly, for a 3-blade turbine, the average Cp values are 0.263 at 200mm, 0.29 at 220mm, 0.34 at 240mm and 0.368 at 260mm blade radii. Beyond the optimal wind speed range, the coefficient of performance tends to decline with increased wind speed. This is because the drag force on blades increases with increased wind speed thereby reducing the lift force. As drag force is proportional to the square of wind velocity, drag force becomes significant at higher wind speeds. This reduces the net lift force generated by blades, reducing the coefficient of performance of turbine.



(A)

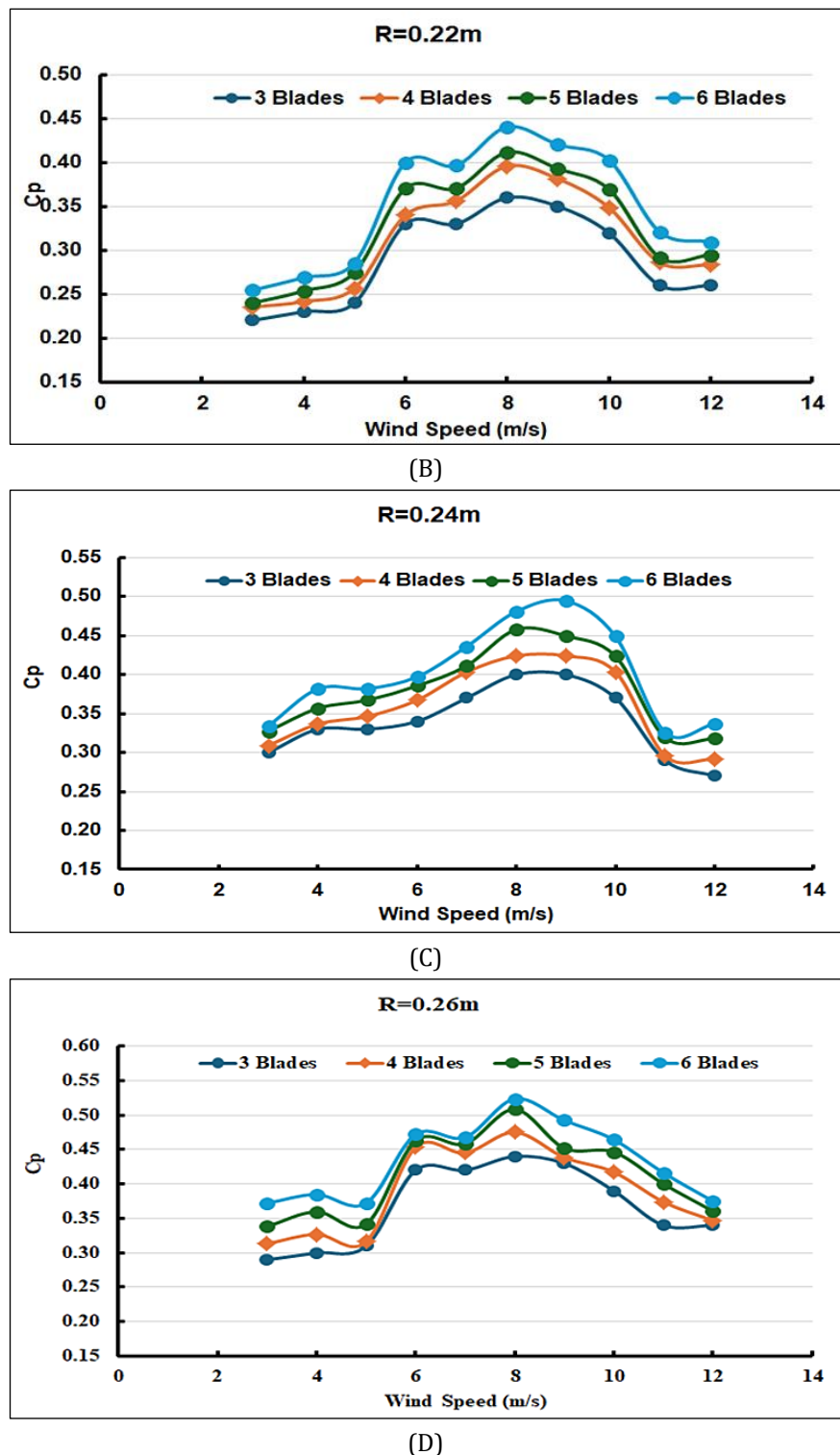


**Figure 4:** Variation of Coefficient of Performance with Wind-Speed with Varying Number of Blades for a Blade Radius of (A) 0.20m, (B) 0.22m, (C) 0.24m and (D) 0.26m

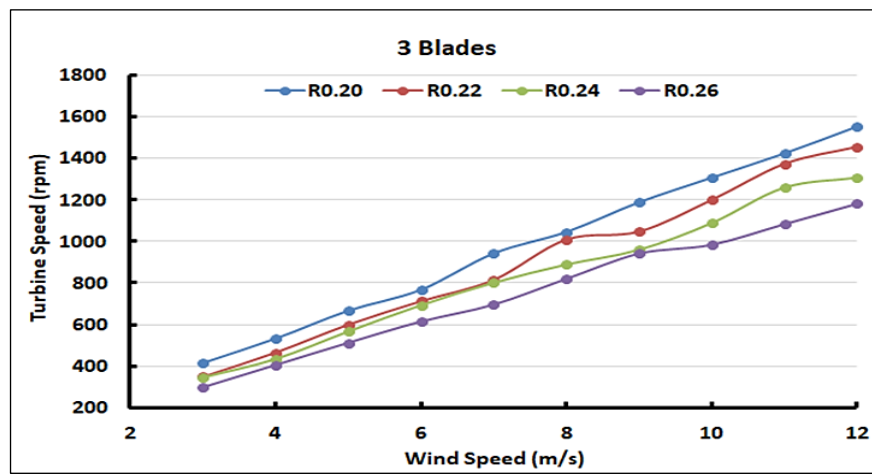
### Turbine Speed

Figures 5(A-D) depict variation of turbine speed with wind speed for a MWT with varying blade radii (R0.2m, R0.22m, R0.24m and R0.26m) and varying blade counts (3-blade, 4-blade, 5-blade and 6-blade). For all turbine configurations, turbine speed increases linearly with wind speed.

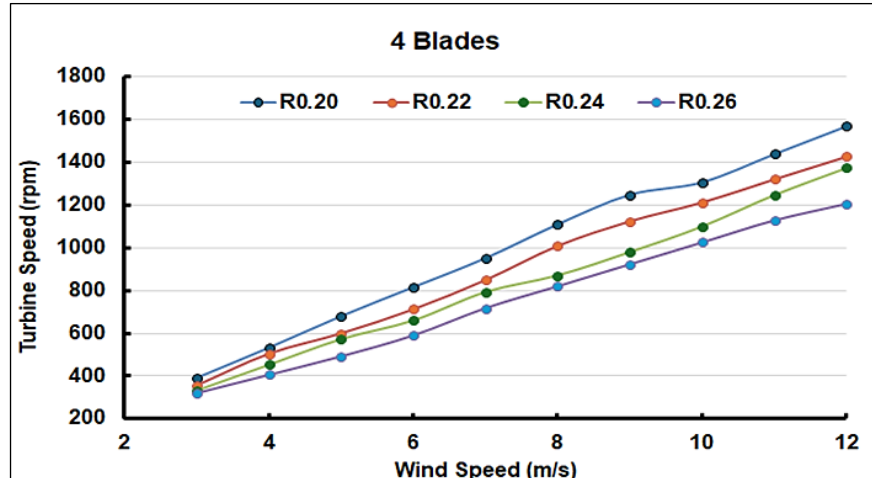
This rise is anticipated due to higher wind speeds delivering higher kinetic energy over blades leading to higher rotational speeds. For example, for a 3-blade turbine with R0.2m, the rotational speed increased to 1552 rpm at a wind speed of 12m/s from 416 rpm at 3 m/s. At a particular wind speed, a turbine with smaller blade radii rotates at

higher speed compared to larger blade radii. Smaller blade radii experience lower aerodynamic drag empowering blades to rotate faster. Additionally, smaller blades typically have a higher lift-to-drag ratio, representing greater efficiency in converting wind energy into rotational motion of blades. As a consequence, the turbine with R0.2m continuously shows higher speed across all turbine configurations. Furthermore, larger blades possess high mass and inertia, which results in retarding the turbine speed. This effect is magnified at higher wind speeds where aerodynamic forces are more significant. Larger blades are subjected to

substantial mechanical and structural stress at higher wind speeds limiting turbine speed to prevent damage. Owing to this effect, the speed difference between turbines with smaller and larger radii is minimal at low wind speeds and becomes more pronounced at higher wind speeds. For instance, a 4-blade turbine rotates at 392 rpm and 320 rpm with a blade radius of 0.2 and 0.26m at lower wind speed (3 m/s) respectively. While at higher wind speed (12 m/s), the smallest and largest turbines rotate at 1568 and 1205 rpm respectively.



(A)



(B)

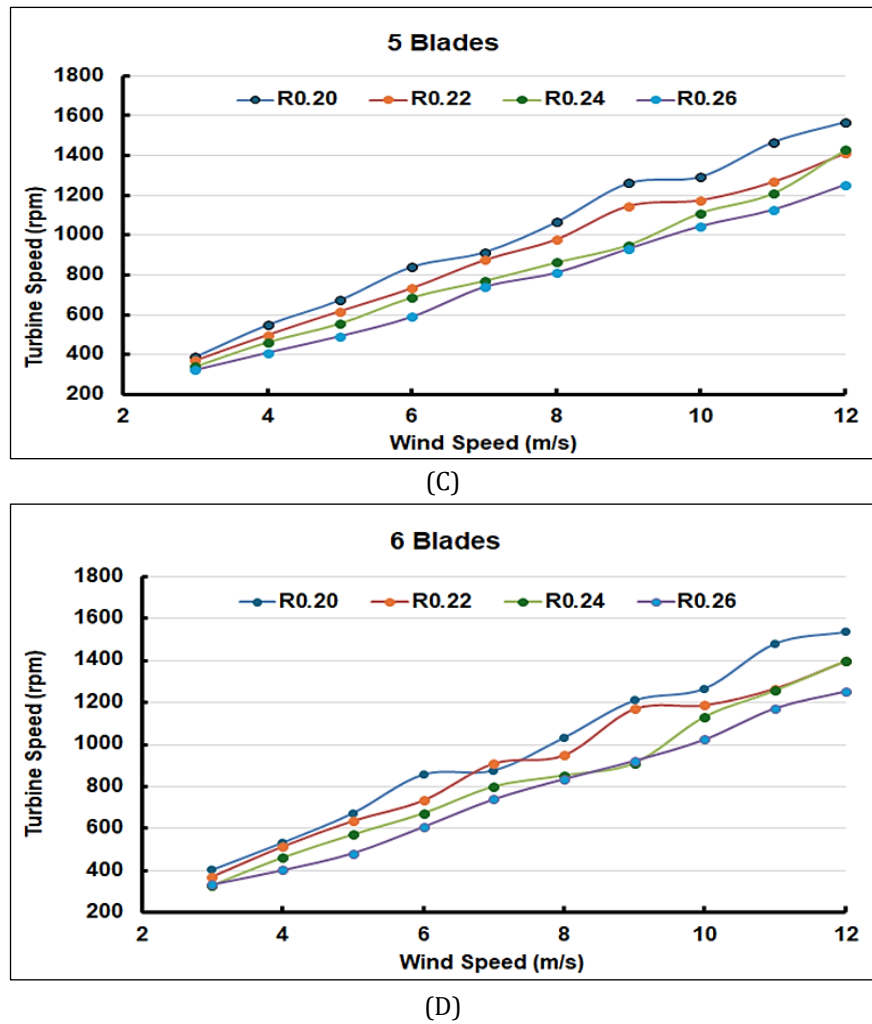


**Figure 5:** Variation of Turbine Speed with Wind Speed with Varying Blade Radii for (A) 3-Blade, (B) 4-Blade, (C) 5-Blade and (D) 6-Blade Configuration

## Conclusion

This study illustrates the significant impact of blade design parameters, such as blade radii, configurations, and the number of blades, on the power generation efficiency of micro-wind turbines (MWTs). Experimental results indicate a non-linear relationship between wind speed and power output, with notable increases observed at elevated wind velocities. The findings emphasize the necessity of optimizing blade geometry and configurations to enhance energy capture, especially in low to moderate wind conditions. This study offers important insights for enhancing the design and efficacy of MWTs, reinforcing their function as sustainable options for decentralized renewable energy production. An increased blade count results in airflow disruption among adjacent blades, thereby disturbing the uniform flow of air. The difference in power generation among turbines with varying blade counts becomes

negligible, yet configurations with a higher number of blades remain advantageous. The turbine generates reduced power output when the  $C_p$  value is lower. As wind velocity increases, a greater proportion of wind energy is transformed into useful power, resulting in an elevated coefficient of performance. The turbine demonstrates increased efficiency within the wind speed range of 6-8 m/s, regardless of blade radii and count, exhibiting a higher  $C_p$ . Increasing the blade count and blade radii positively affects the  $C_p$  at all wind speeds due to the enhanced swept area and blade surface area. The average coefficient of performance values for a turbine with 200mm blade radii across all recorded wind speeds are 0.263, 0.278, 0.292, and 0.31 for configurations with 3, 4, 5, and 6 blades, respectively. For a 3-blade turbine, the average  $C_p$  values are 0.263 at a blade radius of 200mm, 0.29 at 220mm, 0.34 at 240mm, and 0.368 at 260mm. The effect is amplified at increased

wind speeds, as aerodynamic forces become more pronounced. Larger blades experience significant mechanical and structural stress at elevated wind speeds, necessitating a limitation on turbine speed to avert damage. The speed difference between turbines with smaller and larger radii is negligible at low wind speeds but becomes more significant at higher wind speeds. A 4-blade turbine operates at 392 rpm and 320 rpm with blade radii of 0.2 m and 0.26 m, respectively, at a lower wind speed of 3 m/s. At a wind speed of 12 m/s, the smallest and largest turbines operate at rotational speeds of 1568 rpm and 1205 rpm, respectively.

## Abbreviations

ABS: Acrylonitrile Butadiene Styrene, BEM: Blade element momentum, CFD: Computational fluid dynamics, FEA: Finite element analysis, FFD: Free-form deformation, GA: Genetic algorithm, HAWT: Horizontal axis wind turbine, MFO: Moth-flame optimization, MOGA: Multi objective genetic algorithm, MWCNT: Multi walled carbon nanotube, MWT: Micro-wind turbine, PLA: Polylactic acid, TSR: Tip speed ratio, VAWT: Vertical axis wind turbine.

## Acknowledgement

None.

## Author Contributions

All authors contributed equally to this work and played key roles in drafting and revising the manuscript. Finally, all authors have accepted equal responsibility for the entire content of this manuscript and approved its final version.

## Conflict of Interest

The authors declare no conflict of interest.

## Declaration of Artificial Intelligence (AI) Assistance

The authors declare no use of Generative AI and AI Assisted Technologies for the write-up of the manuscript.

## Ethics Approval

Not applicable.

## Funding

This research has not received any external funding.

## References

1. Rathod S, Bond T, Klimont Z, Pierce J, Mahowald N, Roy C, Thompson J, Scott R, Hoal K, Rafaj P. Future PM2.5 emissions from metal production to meet renewable energy demand. *Environmental Research Letters*. 2022;17(4):044043.
2. Holechek J, Geli HME, Sawalhah M, Valdez R. A global assessment: Can renewable energy replace fossil fuels by 2050?. *Sustainability*. 2022;14(8):4792.
3. Shalby M, Salah A, Matarneh G, Marashli A, Gommaa M. An investigation of a 3D printed micro-wind turbine for residential power production. *International Journal Renewable Energy Development*. 2023;12(3):550–559.
4. Alfiansyah R, Sumarjo J. Design of savonius double-stage wind turbine, capacity 300W. *JEEE-U Journal of Electrical and Electronic Engineering-Universitas Muhammadiyah Sidoarjo*. 2023;7(1):11–26.
5. Subrina P, Mayyas M. Wind energy market in USA. *European Journal of Sustainable Development Research*. 2023;7(1):1–14.
6. Claudio-Rodriguez I, Santiago-Vargas A, Espinoza A, Aponte-Roa D. A holistic design approach for a micro wind turbine powertrain. *The American Society of Mechanical Engineers*. Long Beach, California, USA. 2023; POWER2023-108753, V001T05A006:1–8. <https://doi.org/10.1115/POWER2023-108753>
7. MacPhee D, Beyene A. Performance analysis of a small wind turbine equipped with flexible blades. *Renewable Energy*. 2019; 132:497–508.
8. Santoli L, Albo A, Astiaso G, Bruschi D, Cumo F. A preliminary energy and environmental assessment of a micro wind turbine prototype in natural protected areas. *Sustainable Energy Technologies and Assessments*. 2014; 8:42–56.
9. Baghdadi M, Elkoush S, Akle B, Elkhoury M. Dynamic shape optimization of a vertical-axis wind turbine via blade morphing technique. *Renewable Energy*. 2020; 154:239–251.
10. Rodriguez C, Celis C. Design optimization methodology of small horizontal axis wind turbine blades using a hybrid CFD/BEM/GA approach. *Journal of the Brazilian Society of Mechanical Sciences and Engineering*. 2022; 44(6):254.
11. Umar D, Yaw C, Koh S, Tiong S, Alkahtani A, Yusaf T. Design and optimization of a small-

scale horizontal axis wind turbine blade for energy harvesting at low wind profile areas. *Energies*. 2022;15(9):3033.

12. Arivalagan S, Sappani R, Čep R, Kumar M. Optimization and experimental investigation of 3D printed micro wind turbine blade made of PLA material. *Materials*. 2023;16(6):2508.

13. Bekkai R, Laouar R, Mdouki R. Design optimization of three-dimensional geometry of a micro horizontal axis wind turbine blade using the response surface method. *Proceedings in Applied Mathematics and Mechanics*. 2024;24(1):248.

14. Ouyang K, Chen T, You J. Utilizing the Taguchi method to optimize rotor blade geometry for improved power output in ducted micro horizontal-axis wind turbines. *Sustainability*. 2024;16(11):4692.

15. Puttaraju D, Hanumantharaju H, Shreyas, Pradeep, Nuthan. Investigation of bending properties on carbon fiber reinforced polymer matrix composites used for micro wind turbine blades. *Journal of Physics: Conference Series*. 2020;1473:012049.

16. Singh S, Hanumantharaju H, Teja Yadla S, Hemanth R, Srivatsa S. Investigation of bending properties of E-Glass fiber reinforced polymer matrix composites for applications in micro wind turbine blades. *Journal of Physics: Conference Series*. 2020;1473: 012047.

17. Elhenawy Y, Fouad Y, Marouani H, Bassyouni M. Simulation of glass fiber reinforced polypropylene nanocomposites for small wind turbine blades. *Processes*. 2021;9(4):622.

18. Chrysochoidis-Antos N, Amoros A, Van Bussel G, Mertens S, Van Wijk A. Wind resource characteristics and energy yield for micro wind turbines integrated on noise barriers – An experimental study. *Journal of Wind Engineering and Industrial Aerodynamics*. 2020;203:104206.

19. Eltayesh A, Castellani F, Burlando M, Bassily Hanna M, Huzayyin A, El-Batsh H, Becchetti M. Experimental and numerical investigation of the effect of blade number on the aerodynamic performance of a small-scale horizontal axis wind turbine. *Alexandria Engineering Journal*. 2021;60(4):3931–3944.

20. Kadhim H, Resen A, Faraj N. Simulation and experimental study of micro wind turbine rotor blades by using Q-blade software. *AIP Conference Proceedings*. 2022; 2394(1): 090017.

21. Davari H, Kouravand S, Davari M, Kamalnejad Z. Numerical investigation and aerodynamic simulation of Darrieus H-rotor wind turbine at low Reynolds numbers. *Energy Sources, Part A: Recovery, Utilization, and Environmental Effects*. 2023;45(3):6813–6833.

22. Kumar N, Prakash O. Fabrication of exhaust fan cum micro wind turbine and its performance analysis in high-rise building window. *MAPAN-Journal of Metrology Society of India*. 2024; 39(3):601–615.

23. Suresh A, Kumar R, Aljafari B, Thanikanti S. Investigations of the performance of 3D printed micro wind turbine composed of PLA material. *Heliyon-A Cell Press Journal*. 2024; 10(3):1-15.

24. Hansen C, Hansen K. Recent advances in wind turbine noise research. *Acoustics*. 2020; 2:171–206.

25. Eftekhari H, Mahdi Al-Obaidi A, Eftekhari S. Aerodynamic performance of vertical and horizontal axis wind turbines: A comparison review. *Indonesian Journal of Science & Technology*. 2022; 7(1):65-88.

**How to Cite:** Ghane DB, Wakchaure VD Experimental Analysis of Micro-Wind Turbine Performance: Blade Geometry and Wind Speed Interactions. *Int Res J Multidiscip Scope*. 2026; 7(1): 1337-1350.  
DOI: 10.47857/irjms.2026.v07i01.08331